J Solid State Electrochem (2012) 16:1877–1881
DOI 10.1007/s10008-011-1545-y

ORIGINAL PAPER

Cycling effects on interfacial reliability of TiO_2 anode film in thin film lithium-ion microbatteries

Jing Zhu · Kaiyang Zeng · Li Lu

Received: 27 July 2011 / Revised: 22 August 2011 / Accepted: 26 August 2011 / Published online: 8 September 2011

Abstract This work presents a comprehensive study on the cycling effects on morphological, nanomechanical, and interfacial properties of sputtered TiO_2 anode film during discharge/charge cycling. TiO_2 film mechanically fails due to the repeated volume change and related generation/relaxation of stress induced by electrochemical phase transformation. The induced stress intensifies the initiation/propagation of cracks, also the interfacial delamination. Both morphology and mechanical property changes have harmful effects on the electrical contact, resulting in the battery aging. This paper also demonstrates that the experiment and analysis method is effective to characterize the interfacial reliability within thin film microbatteries.

Keywords Thin film lithium-ion battery · TiO_2 · Nanoindentation · Interfacial reliability

Introduction

Lithium-ion batteries have attracted much attention due to high energy density, long cycle life, and little memory effect. Advances in MEMS technologies reduce the size, current density, and power requirements of electronic devices to lower levels, promoting the development of thin film microbatteries, which have special applications in semiconductor chips, implanted medical devices, and integrated circuits [1, 2]. Although prolonging battery life has become more significant, the investigation of aging mechanism is still very challenging since capacity fading originates from various interrelated processes. Apart from electrochemical issues, underlying aging phenomenon can be related to the mechanical failure due to volume change and lattice distortion induced by Li^+ insertion/extraction and the related generation/relaxation of intercalation-induced stress [3–5]. Currently, microbattery technology is in the transition from traditional electrochemistry to solid-state physics; interfacial reliability of electrode film has become a critical issue due to its significant roles in both structural integrity and cycling performance of thin film batteries [6, 7]. However, previous studies have less concern on these issues since the quantification of interfacial reliability is not simple, requiring not only practical experimental method but also theoretical analysis on solid adhesion mechanics [8–10]. Therefore, using the experimental and analysis method developed in the previous study [11], this combined study has investigated the cycling effects on surface morphology, nanomechanical, and interfacial reliability of TiO_2 anode film using various characterization techniques, which can give a comprehensive insight into the aging mechanism of TiO_2 anode film, providing a new perspective to understand the thin film battery aging also.

Experimental procedure

TiO_2 film was deposited on Ti substrate by dc sputtering using a titanium target at a power of 100 W in Ar/O_2 (3:1) atmosphere at room temperature. The pure Ti substrate (1 cm diameter and 1 mm thick) was previously autopolished to a mirror-like surface (by alumina polishing agent). Film thickness was measured by surface profilometer as 150 nm. Microstructure of film was characterized by X-ray

J. Zhu (✉) · K. Zeng · L. Lu
Department of Mechanical Engineering,
National University of Singapore,
9 Engineering Drive 1,
Singapore 117576, Singapore
e-mail: g0800346@nus.edu.sg

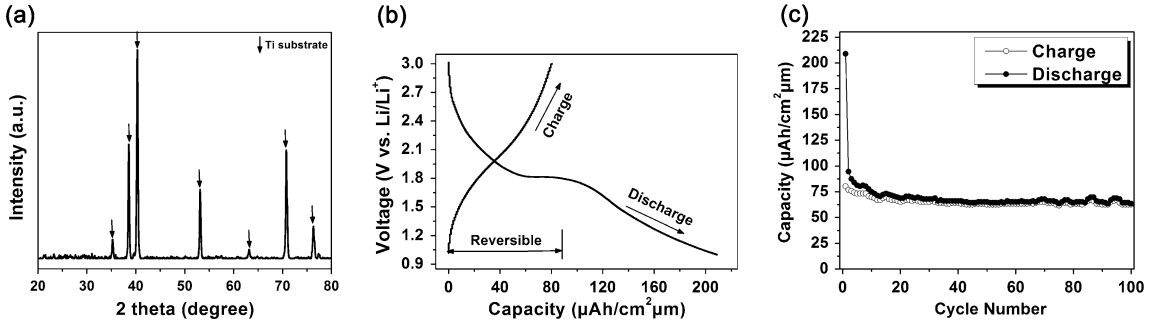

Fig. 1 **a** XRD pattern of as-deposited TiO_2 anode film on Ti substrate, **b** the first discharge/charge curves, and **c** cycling performance of TiO_2 anode film up to 100 cycles

diffraction (XRD). The two-electrode half-cell using TiO_2 film as working electrode and Li metal foil as counter electrode was assembled in an Ar-filled glove box. The electrolyte was 1-M $LiPF_6$ (EC/DEC) solution. Galvanostatic discharge/charge cycling was conducted with a voltage of 0.01–2.5 V at a constant current density of 15 μA cm^{-2} using Neware battery tester. Atomic force microscopy (AFM) was conducted in tapping mode using a silicon tip with spring constant of 2 Nm^{-1} to study the topography changes during cycling. Surface roughness can be quantitatively measured by root-mean-squared roughness (RMS) determined by AFM program.

Elastic modulus and nanohardness were determined by nanoindenter with continuous stiffness measurement option and standard Berkovich indenter tip under the strain rate control (0.05 s^{-1}). Wedge indentations, conducted by another nanoindenter using 90° diamond wedge tip under load control, were used to induce the interfacial delamination. To characterize the interfacial crack profile, focused ion beam (FIB) was used to make cross-sectional cuttings. The cross-sectional and plain view images of interfacial delamination can be captured by FIB and field-emission scanning electron microscopy (FESEM), respectively.

Results and discussions

Structural and electrochemical characterization

Figure 1a shows the XRD pattern of TiO_2 film on Ti substrate deposited at room temperature. There is no detectable peak of TiO_2 except the diffraction peaks of Ti substrate (marked by arrows), indicating that TiO_2 film is poorly crystalline (nanocrystalline). This is similar to the findings in previous studies [12]. Figure 1b shows the initial discharge/charge curves for TiO_2 anode film, indicating a distinct discharge plateau at about 1.75 V vs. Li/Li^+, which is in well agreement with the typical

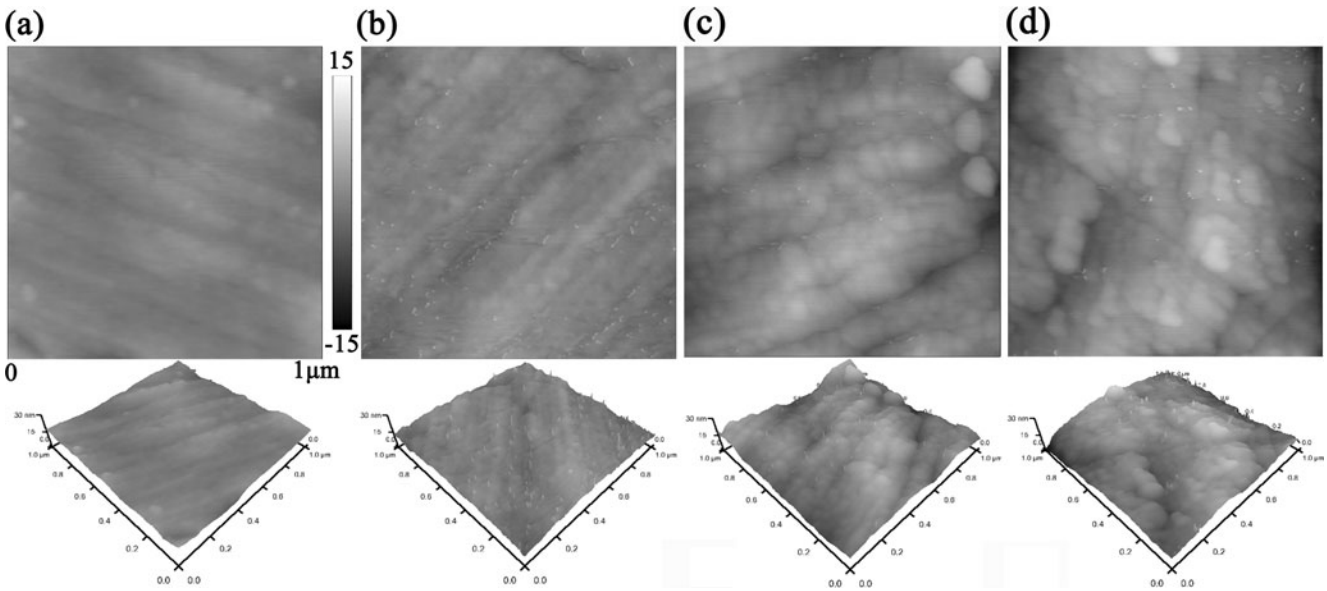

Fig. 2 AFM topography of **a** deposited, **b** 10 cycled, **c** 50 cycled, and **d** 100 cycled TiO_2 film

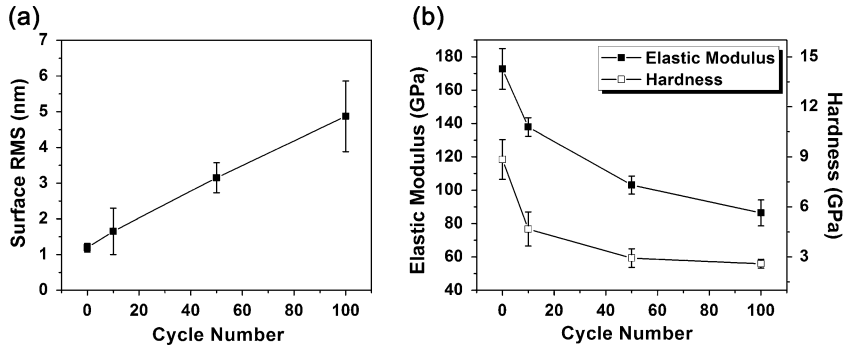

Fig. 3 **a** Surface roughness measured by AFM and **b** calculated elastic modulus and nanohardness of TiO_2 anode film at different cycling stages

electrochemical characteristic of TiO_2 anode. The electrochemical reaction for TiO_2 on Li^+ insertion/extraction can be written as [13, 14]:

$$TiO_2 + xLi^+ + xe^- \rightleftarrows Li_xTiO_2 \quad (1)$$

As shown in Fig. 1c, nanocrystalline TiO_2 anode film shows large discharge/charge capacity and excellent cycling stability up to 100 cycles. However, there is a large irreversible capacity loss in the initial cycle, which is attributed to several phenomena: (a) the formation of solid electrolyte interface film accompanied by the irreversible consumption of Li^+ and (b) severe side reaction related to larger contact area and shorter diffusion length in thin film electrode [15].

Surface topography

Figure 2 shows both 2D and 3D AFM topography of TiO_2 film at different cycling stages. There is an observable volume expansion with the increase of cycling number, especially after 50 cycles. The film shows bumping and rough surface due to Li^+ irreversible insertion. As shown in Fig. 2c, d, microcracks can be induced by the film contraction upon Li^+ extraction. These cracks have harmful effects on the electrical contact between anode film and the substrate, resulting in a rise in impedance and a reduction of capacity [16, 17]. In addition, nonuniformity is observed due to the agglomeration of nanograins, which may be induced by the electrochemical migration. The surface topography changes also lead to an increase in surface roughness in terms of RMS (Fig. 3a) since TiO_2 anode film cannot return to the original volume upon Li^+ extraction due to the poor crystallinity accompanied by the surface Li^+ absorption.

Nanomechanical and interfacial reliability

The elastic modulus and hardness of TiO_2 films are determined by analyzing nanoindentation load-displacement (*P*–*h*) curves [18, 19]. Figure 3b shows that both elastic modulus and nanohardness decrease with the increase of cycling number. Furthermore, Fig. 4 compares *P*–*h* curves at different cycling stages. The displacement steadily increases at the same load with the increase of cycling number. This is mainly due to the decrease of hardness since the indentation measures the penetration resistance to the compressive intrusion of indenter tip [20]. Upon the discharging of TiO_2/Li half-cell, the migration of Li^+ into TiO_2 requires a volume expansion of anode film. This volume expansion is constrained by the rigid substrate, resulting in compressive stress in the film. Li^+ is removed from the anode upon charging, introducing porosity into the film, which can relax the compressive stress more rapidly than the delithiation process [21, 22]. Thus, further delithiation process leads to a volume contraction, inducing tensile stress in the film. In addition, Li^+ insertion/extraction into TiO_2 anode film leads to the lattice parameter change and crystal distortion, inducing further

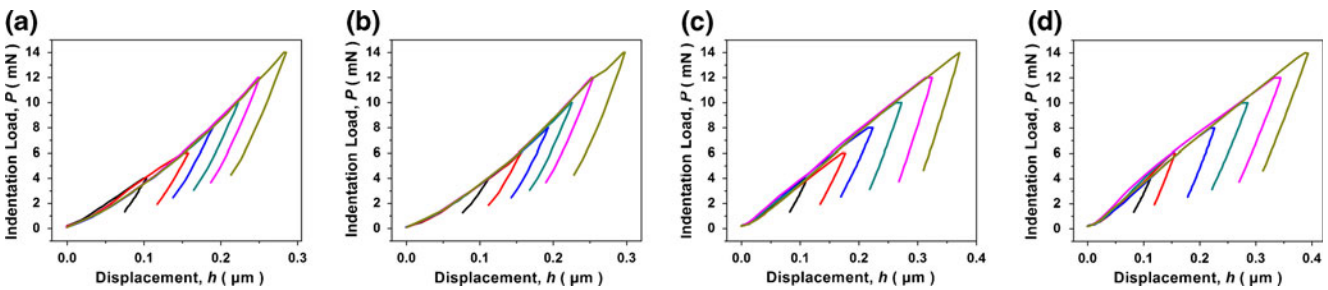

Fig. 4 *P*–*h* curves of **a** deposited, **b** 10 cycled, **c** 50 cycled, and **d** 100 cycled TiO_2 film

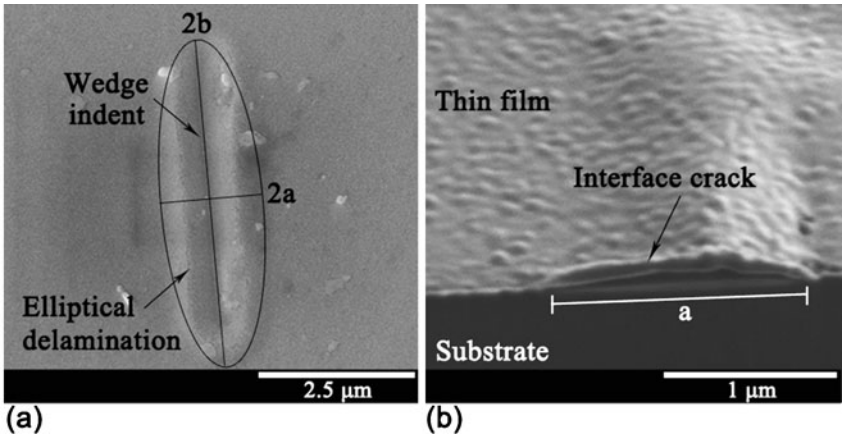

Fig. 5 **a** FESEM plain view and **b** FIB cross-sectional view images of interface delamination

stress and strain to the nanograins. The induced stress accumulates over cycles finally surpassing the strength of anode material, causing fracture and microcracking. Thus, after discharge–charge cycle, the intercalation-induced stress together with microcracks can lead to the mechanical degradation of TiO_2 anode film.

Combining FESEM plain view and FIB cross-sectional view images of wedge indentation impression (Fig. 5a, b), when the indentation load is higher than a critical value, i.e., 6 mN for as-deposited film, 4 mN for cycled film, the interfacial delamination occurs at the penetration depth of about 100 nm. The interface toughness can be calculated as described previously [11]. As summarized in Table 1, there is a considerable decrease of interface toughness during 100 cycles. This is mainly attributed to the reduction of elastic modulus since the indentation-induced stress is proportional to the elastic modules (Fig. 3b). Apart from this, porosities and cracks induced by lithiation/delithiation also play significant roles; the denser as-deposited film has higher interface toughness than cycled films. Since the crack propagation is more difficult through compressive stress field, the tensile stress after discharge/charge cycling also enhances the interfacial delamination; anode film is more likely to detach from the substrate [23]. It is noted that the decreases in elastic modulus, hardness, and interfacial toughness are more significant during the first 10 cycles, corresponding to the larger capacity fading during the initial cycles. Furthermore, according to our previous study [24], rutile RuO_2 anode film with worse cycling performance and surface morphology stability shows more significant degradation in both nanomechanical properties and interfacial reliability. Therefore, there is a relationship between the capacity fading and nanomechanical degradation of anode film within lithium-ion batteries.

Conclusions

In this study, TiO_2 films have been fabricated by reactive sputtering and investigated as anode for lithium-ion batteries, which expand with Li^+ insertion and contract with Li^+ removed, accompanying with a rise in surface roughness. Mechanical stress induced by volume expansion/contraction drives the initiation/propagation of microcracks, also enhancing the interfacial delamination. Electrochemical phase transformations also take place, which induce lattice distortion and further mechanical stress, leading to the mechanical degradation at nanoscale. Both mechanical degradation and interfacial delamination have harmful effects on the electrical contact of electrode film, reducing the battery life. This study has clearly shown the electrochemical cycling effects on morphological, nanomechanical, and interfacial properties of TiO_2 anode, providing a new perspective for

Table 1 Average value of interface toughness and key parameters for TiO_2 anode film

	Short axis crack length, $2a$ (μm)	Indentation plastic depth, h_p (μm)	Indentation-induced stress, σ_0 (MPa)	Critical buckling stress, σ_c (MPa)	Interface toughness, Γ_i (J/m^2)
Deposited	0.94±0.03	0.063±0.002	2683.06±85.81	15535.61±999.78	2.75±0.17
10 cycled	1.07±0.03	0.063±0.001	1862.36±37.65	9493.37±573.99	1.66±0.07
50 cycled	1.33±0.03	0.072±0.001	1479.16±38.81	4578.16±179.54	1.40±0.07
100 cycled	1.45±0.04	0.071±0.002	1112.10±32.21	3250.75±191.12	0.95±0.05

Critical loads, P_{max}, for as-deposited are 6 mN; for 10th, 50th, and 100th cycled films, the critical loads are 4 mN

understanding the thin film battery aging. This study also demonstrates that nanoindentation experiment and related analysis method is proved effective to quantify interfacial reliability within thin film microbatteries.

Acknowledgments This work is supported by the Agency for Science, Technology and Research (A*Star), Singapore on research project 0721340051 (R-265-000-292-305) and the Ministry of Education, Singapore, through the National University of Singapore under Academic Research Funds (R265-000-305-112).

References

1. Patil A, Patil V, Wook Shin D, Choi J-W, Paik D-S, Yoon S-J (2008) Issue and challenges facing rechargeable thin film lithium batteries. Mater Res Bull 43(8–9):1913–1942
2. Souquet JL, Duclot M (2002) Thin film lithium batteries. Solid State Ion 148(3–4):375–379
3. Aurbach D, Zinigrad E, Cohen Y, Teller H (2002) A short review of failure mechanisms of lithium metal and lithiated graphite anodes in liquid electrolyte solutions. Solid State Ion 148(3–4):405–416
4. Swiatowska-Mrowiecka J, Maurice V, Klein L, Marcus P (2007) Nanostructural modifications of V2O5 thin films during Li intercalation studied in situ by AFM. Electrochem Commun 9 (9):2448–2455
5. Vetter J, Novák P, Wagner MR, Veit C, Möller KC, Besenhard JO, Winter M, Wohlfahrt-Mehrens M, Vogler C, Hammouche A (2005) Ageing mechanisms in lithium-ion batteries. J Power Sourc 147:269–281
6. Bates JB, Dudney NJ, Neudecker B, Ueda A, Evans CD (2000) Thin-film lithium and lithium-ion batteries. Solid State Ion 135:33–45
7. Ritchie AG (2004) Recent developments and likely advances in lithium rechargeable batteries. J Power Sourc 136(2):285–289
8. Boer MPd, Gerberich WW (1996) Microwedge indentation of the thin film fine line-II. Experiment. Acta Mater 44:3177–3187
9. Boer MPd, Gerberich WW (1996) Microwedge indentation of thin film fine line-I. mechanics. Acta Mater 44:3169–3175
10. Volinsky AA, Gerberich WW (2003) Nanoindentation techniques for assessing mechanical reliability at the nanoscale. Microelectron Eng 69(2–4):519–527
11. Zhu J, Yeap KB, Zeng K, Lu L (2011) Nanomechanical characterization of sputtered RuO_2 thin film on silicon substrate for solid state electronic devices. Thin Solid Films 519(6):1914–1922
12. Ortiz GF, Hanzu I, Knauth P, Lavela P, Tirado JL, Djenizian T (2009) TiO_2 nanotubes manufactured by anodization of Ti thin films for on-chip Li-ion 2D microbatteries. Electrochim Acta 54 (17):4262–4268
13. Wang Y, Wu M, Zhang WF (2008) Preparation and electrochemical characterization of TiO_2 nanowires as an electrode material for lithium-ion batteries. Electrochim Acta 53(27):7863–7868
14. Wu M-S, Wang M-J, Jow J-J, Yang W-D, Hsieh C-Y, Tsai H-M (2008) Electrochemical fabrication of anatase TiO_2 nanostructure as an anode material for aqueous lithium-ion batteries. J Power Sourc 185(2):1420–1424
15. Sarre G, Blanchard P, Broussely M (2004) Aging of lithium-ion batteries. J Power Sourc 127(1–2):65–71
16. Moon HS, Lee W, Reucroft PJ, Park JW (2003) Effect of film stress on electrochemical properties of lithium manganese oxide thin films. J Power Sourc 119–121:710–712
17. Mukaibo H, Momma T, Mohamedi M, Osaka T (2005) Structural and morphological moditications of a nanosized 62 atom percent Sn-Ni thin film anode during reaction with lithium. J Electrochem Soc 152(3):A560–A565
18. Joslin DL, Oliver WC (1990) A new methode for analyzing data from continuous depth-sensing microindentation tests. J Mater Res 5(1):123–126
19. Oliver WC, Pharr GM (1992) An improved thechnique for determination hardness and elastic-modulus using load and displacement sensing indentation experiments. J Mater Res 7 (6):1564–1583
20. Chen Z, He M, Balakrisnan B, Chum CC (2006) Elasticity modulus, hardness and fracture toughness of Ni3Sn4 intermetallic thin films. Mat Sci Eng A 423:107–110
21. Chen J, Bull SJ, Roy S, Kapoor A, Mukaibo H, Nara H, Momma T, Osaka T, Shacham-Diamand Y (2009) Nanoindentation and nanowear study of Sn and Ni-Sn coatings. Tribol Int 42:779
22. Mukaibo H, Momma T, Shacham-Diamand Y, Osaka T, Kodaira M (2007) In situ stress transition observations of electrodeposited Sn-based anode materials for lithium-ion secondary batteries. Electrochem Solid State Lett 10(3):A70–A73
23. Cibert C, Hidalgo H, Champeaux C, Tristant P, Tixier C, Desmaison J, Catherinot A (2008) Properties of aluminum oxide thin films deposited by pulsed laser deposition and plasma enhanced chemical vapor deposition. Thin Solid Films 516(6):1290–1296
24. Zhu J, Zeng K, Lu L (2011) Cycling effect on morphological and interfacial properties of RuO2 anode film in thin-film lithium ion microbatteries. Metall Matter Trans 1–9. doi:10.1007/s11661-011-0847-0